

Molecular Structure and Spectroscopic Signatures of Acrolein: Theory Meets Experiment

Cristina Puzzarini,^{*,†} Emanuele Penocchio,^{†,‡} Malgorzata Biczysko,^{‡,§} and Vincenzo Barone^{*,‡}

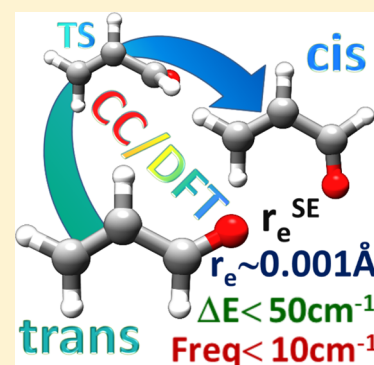
[†]Dipartimento di Chimica "Giacomo Ciamician", Università di Bologna, Via Selmi 2, I-40126 Bologna, Italy

[‡]Scuola Normale Superiore, Piazza dei Cavalieri 7, I-56126 Pisa, Italy

[§]Consiglio Nazionale delle Ricerche, Istituto di Chimica dei Composti OrganoMetallici (ICCOM-CNR), Area della Ricerca CNR, UOS di Pisa, Via G. Moruzzi 1, I-56124 Pisa, Italy

S Supporting Information

ABSTRACT: A comprehensive study of the molecular structure and IR spectrum of *cis* and *trans* acrolein has been performed by an integrated computational approach coupling methods rooted in the coupled-cluster ansatz and the density functional theory. From the one side, DFT anharmonic force fields allow us to determine very reliable semi-experimental structures for both isomers, which are in remarkable agreement with the geometries issuing from CCSD(T) computations accounting for the extrapolation to the complete basis set and core correlation. The same kind of coupled-cluster computations provide dipole moment, relative energies, and interconversion barrier in remarkable agreement with experiments. Finally, harmonic CCSD(T) results coupled to DFT evaluation of mechanical and electrical anharmonicity allow us, in the framework of second-order perturbative vibrational theory, to confirm most of the experimental assignments of IR spectra, and to suggest some additional interpretations for congested regions including fundamental bands together with overtones and combination bands.



INTRODUCTION

Propenal (CH₂CHCHO), better known as acrolein, is the simplest member of the α,β -unsaturated aldehyde family, an extremely varied class of compounds, whose photochemistry is of great interest. It may be formed from the breakdown of certain pollutants in outdoor air, from the incomplete combustion of organic materials, and it arises endogenously in human beings as a metabolic byproduct.¹ It is toxic to humans by inhalation, oral, or dermal exposures but has significant industrial applications as biocide and building block to other chemical compounds, such as acrylic acid and the methionine amino acid.¹ The electrophilic properties of acrolein play a prominent role in the mechanism of reactions with DNA bases. Moreover, due to its nature of bifunctional electrophile, acrolein–DNA adducts show a tendency to cyclization. Acrolein is also a molecule of astrophysical interest; in fact, the *trans* form of acrolein has been detected toward the star-forming region Sagittarius B2(N) by Hollis et al.² through the observation of rotational transitions using 100 m Green Bank Telescope (GBT) operating in the frequency range from 18.0 to 26.0 GHz.

Acrolein exists in two forms, *cis* and *trans*, which refer to the position of the oxygen atom with respect to the –CH₂ group involved in the double bond. Spectroscopic measurements in the microwave,^{3,4} infrared,⁵ and near-ultraviolet^{6,7} regions have confirmed that the *trans* form is the most stable, and thus, the most abundant conformer of acrolein. The first spectroscopic evidence of the less abundant *cis* conformer in the gas phase was found in studies of the near-ultraviolet spectrum.^{8,9} Later,

cis-acrolein was detected in argon matrices^{10,11} and in the gas phase Raman spectrum.¹² The first microwave observation of the *cis* form was reported by Blom and Bauder.¹³ They have reported the ground-state rotational and quartic centrifugal-distortion constants as well as the dipole moment values. The dipole moments have been found to be $\mu = 3.117 \pm 0.004$ D and $\mu = 2.552 \pm 0.003$ D for *trans* and *cis*,^{13,14} respectively. The availability of all monosubstituted isotopologues allowed for the measurement of the corresponding rotational spectra and the determination of a complete substitution structure (r_s) for both conformers. Winnewisser et al.¹⁵ extended the analysis of the ground state of the *trans* form to the millimeter wave region up to 180 GHz, thus yielding an improved and extended set of ground-state rotational and centrifugal distortion constants. Recently, Jaman and Bhattacharya¹⁶ investigated the rotational spectra of the lowest torsional levels. After nearly complete determinations of the fundamental transitions in the infrared (IR) spectra of both conformers performed more than 30 years ago,^{17,18} further analyses of the far-infrared spectrum of *trans*-acrolein including overtones and combination bands were reported in the last years^{19,20} together with a structural determination based on NMR spectroscopy.²¹ Furthermore, the difference between the acrolein conformers in the gas phase

Special Issue: Franco Gianturco Festschrift

Received: April 14, 2014

Revised: May 14, 2014

Published: May 19, 2014

($660 \pm 40 \text{ cm}^{-1}$) was derived from the temperature dependence of the intensities of electronic-vibrational spectrum bands.^{8,22}

Several quantum-chemical computations^{16,21,23–27} have paralleled the experimental work, but none of them employed the state-of-the-art methods, which are nowadays able to provide for small- to medium-sized molecules structures and spectroscopic parameters rivaling the most sophisticated experimental techniques (see, for example, refs 28–34). It is the purpose of the present study to fill this gap by means of an integrated approach based on the coupled-cluster (CC) ansatz, together with the extrapolation to complete basis set (CBS) limit and inclusion of core–valence (CV) correlation effects for energies and structures. Methods rooted in the density functional theory (DFT) are used to evaluate anharmonic contributions and vibrational effects by means of the recently introduced general second-order vibrational perturbative treatment (GVPT2) approach to compute vibrational corrections and transition moments.^{35,36} At the same time, we improve the molecular structure determination for both conformers by deriving the so-called semiexperimental structure (r_e^{SE}) in which experimental rotational constants are first converted to equilibrium constants using computed vibration–rotation interaction constants and then employed in a least-squares fitting of geometrical parameters.^{30,37–40}

METHODOLOGY

In geometry optimizations, equilibrium energy and molecular property evaluations, and harmonic force-field computations, the coupled-cluster (CC) level of theory employing the CC singles and doubles (CCSD) approximation augmented by a perturbative treatment of triple excitations (CCSD(T))⁴¹ was mainly employed in conjunction with the correlation-consistent, (aug)-cc-p(C)VnZ ($n = T, Q$), basis sets.^{42–44} All CC calculations were carried out with the quantum-chemical CFour program package.⁴⁵ DFT was used in geometry optimizations as well as to compute harmonic and anharmonic force fields. Within the DFT approach, the double-hybrid B2PLYP^{46,47} functional was considered in conjunction with the aug-cc-pVTZ basis set because of its well-proved accuracy.⁴⁸ All DFT and VPT2 computations were performed employing a locally modified version of the GAUSSIAN suite of programs for quantum chemistry.⁴⁹

Molecular Structure. In molecular structure determination, for both conformers, basis-set effects as well as core-correlation contributions were taken into account simultaneously at an energy-gradient level by making use of the composite quantum-chemical scheme presented in refs 28 and 29. The contributions considered are the Hartree–Fock self-consistent-field (HF-SCF) part extrapolated to the CBS limit, the valence correlation energy at the CCSD(T) level extrapolated to CBS, and the core–valence correlation correction. The overall gradient employed in the geometry optimization was therefore given by

$$\frac{dE_{\text{CBS+CV}}}{dx} = \frac{dE^{\infty}(\text{HF-SCF})}{dx} + \frac{d\Delta E^{\infty}(\text{CCSD(T)})}{dx} + \frac{d\Delta E(\text{CV})}{dx} \quad (1)$$

where $dE^{\infty}(\text{HF-SCF})/dx$ and $d\Delta E^{\infty}(\text{CCSD(T)})/dx$ are the energy gradients corresponding to the $\exp(-Cn)$ extrapolation scheme for the HF-SCF energy⁵⁰ and to the n^{-3} extrapolation

formula for the CCSD(T) correlation contribution,⁵¹ respectively. In the expression given above, $n = T, Q$, and 5 were chosen for the HF-SCF extrapolation, and $n = T$ and Q were used for CCSD(T). The core-correlation energy correction, $\Delta E(\text{CV})$, was obtained as difference of all-electron and frozen-core CCSD(T) calculations using the core–valence cc-pCVTZ basis set.^{44,52}

The molecular structures of the *trans* and *cis* conformers were also optimized at the B2PLYP/aug-cc-pVTZ level together with that of the transition state for the isomerization reaction.

Thanks to the availability of the ground-state rotational constants for all monosubstituted isotopologues,¹⁴ the so-called semiexperimental structure was determined for both conformers. This required to carry out a least-squares fit of the molecular structural parameters to the equilibrium moments of inertia, I_c^i . The latter were straightforwardly obtained from the corresponding equilibrium rotational constants, B_c^i , which in turn were derived from the experimental ground-state constants, B_0^i , by correcting them for vibrational and electronic effects:⁵³

$$B_c^i = B_0^i + \frac{1}{2} \sum_r \alpha_r^i - \Delta B_{\text{el}}^i \quad (2)$$

In the fitting procedure, all moments of inertia were equally weighted.

In eq 2, $(1/2) \sum_r \alpha_r^i$ is the vibrational correction, where α_r^i are the computed vibration–rotation interaction constants, with r and i denoting the normal mode and the inertial axis, respectively. These constants were obtained by means of vibrational second-order perturbation theory (VPT2).⁵³ The required cubic force fields were obtained at the B2PLYP/aug-cc-pVTZ level of theory from numerical differentiation of analytical second-order derivatives.⁴⁸

In eq 2, the electronic corrections to rotational constants, ΔB_{el}^i , are due to the electronic-distribution contribution to the moments of inertia and are thus connected to the rotational g -factor (for the corresponding theory, see for example refs 30, 54, and 55):

$$\Delta B_{\text{el}}^i = \frac{m_e}{m_p} g^i B_c^i \quad (3)$$

In the equation above, m_e and m_p are the mass of the electron and proton, respectively, and g^i denotes the diagonal element of the rotational g -factor along the i inertial axis. For all isotopic species considered, the latter were computed at the B3LYP/aug-cc-pVTZ level.

Energetics and Molecular Properties. For the determination of the conformational enthalpy, a composite scheme^{56–59} was employed. The total energies were obtained by the following formula:

$$E_{\text{tot}} = E_{\text{HF-SCF}}^{\infty} + \Delta E_{\text{CCSD(T)}}^{\infty} + \Delta E_{\text{CV}} + \Delta E_{\text{fT}} + \Delta E_{\text{pQ}} \quad (4)$$

where the effects due to a full treatment of triples (fT) and a perturbative treatment of quadruple excitations (pQ) were also accounted for. The corresponding corrections were obtained as differences between CCSDT and CCSD(T) and between CCSDT(Q) and CCSDT in frozen-core calculations employing the cc-pVTZ and cc-pVDZ basis sets, respectively. CCSDT stands for the full CC singles, doubles, and triples^{60–62} and CCSDT(Q) for the CCSDT augmented by a perturbative

Table 1. Equilibrium Structure (Distances in Å, Angles in degrees) and Dipole Moment (debye) of *trans*-Acrolein

| parameters | this work | | | experiment |
|----------------------|--------------------|----------------------------|----------------------------|-----------------------|
| | B2PLYP/aug-cc-pVTZ | best ^a estimate | semiexp ^b r_e | r_s^c |
| C1–O ₄ | 1.2135 | 1.2096 | 1.2105(1) | 1.214(4) |
| C1–C2 | 1.4696 | 1.4704 | 1.4700(1) | 1.468(4) |
| C2–C3 | 1.3342 | 1.3348 | 1.3356(2) | 1.340(4) |
| C1–H5 | 1.1067 | 1.1055 | 1.1049(2) | 1.113(6) |
| C2–H6 | 1.0816 | 1.0817 | 1.0815(1) | 1.084(5) |
| C3–H7 | 1.0826 | 1.0829 | 1.0827(2) | 1.090(4) |
| C3–H8 | 1.0797 | 1.0797 | 1.0792(2) | 1.080(3) |
| C2–C1–O ₄ | 124.28 | 124.05 | 123.99(1) | 124.0(6) |
| C3–C2–C1 | 120.66 | 120.21 | 120.22(1) | 119.7(3) |
| C2–C1–H5 | 114.84 | 114.98 | 115.02(2) | 114.7(5) |
| C3–C2–H6 | 122.47 | 122.74 | 122.76(2) | 122.4(4) |
| C2–C3–H7 | 120.66 | 120.45 | 120.43(1) | 120.4(5) |
| C2–C3–H8 | 122.17 | 122.11 | 122.09(2) | 122.2(5) |
| μ_d | 3.364 | 3.205 ^d | | |
| μ_0^{298} | 3.264 | 3.105 ^e | | 3.117(4) ^f |

^aBest estimate from eq 1. ^b B_0 from ref 14 (parent species: ref 16) and vibrational corrections at the B2PLYP/aug-cc-pVTZ level. Given uncertainties are 3 times the standard deviation of the fit. ^cSubstitution structure, ref 14. ^dEquilibrium values computed at the best-estimated structure using the CCSD(T)/aug-cc-pVQZ level of theory. ^eEquilibrium values of footnote *d* corrected for vibrational and temperature effects at the B2PLYP/aug-cc-pVTZ level. ^fReference 14.

treatment of quadruple excitations.^{63,64} CCSDT(Q) computations were carried out with the MRCC package⁶⁵ by Kállay interfaced to CFour. The best-estimated equilibrium geometry mentioned above was used for the energy calculations.

The extrapolation to the CBS limit and core-correlation contribution in eq 4 were obtained with the same basis sets used for the molecular structure determination, whereas zero-point vibrational (ZPV) energies for both *trans* and *cis* forms were determined from B2PLYP/aug-cc-pVTZ force fields, using the resonance-free formulation proposed by Schuurman et al.⁶⁶ and recently generalized toward transition states.⁶⁷

In view of establishing an accurate energy barrier for the *trans*–*cis* interconversion, single-point energy calculations at the B2PLYP/aug-cc-pVTZ optimized geometries (*trans*, *cis*, and transition state) were carried out at the CCSD(T)/CBS+CV level of theory. CBS and CV denote the extrapolated total energy and the core–valence correlation correction, respectively, according to eqs 1 and 4.

For both the conformers, the components of the molecular electric dipole moment were computed at the CCSD(T)/aug-cc-pVQZ level (within the frozen core approximation), employing the best-estimated equilibrium structure, and at the B2PLYP/aug-cc-pVTZ level at the corresponding optimized geometry. The vibrational corrections were evaluated by performing a vibrational averaging⁶⁸ of the molecular property by means of second-order perturbation theory and with anharmonic vibrational nuclear wave functions.^{69–71} The geometrical dependence of a molecular property is included within the model by expanding it in a Taylor series around the equilibrium structure. In this framework, the averaged property, as a function of the normal coordinates, is expressed as the sum of the purely electronic property and a temperature-dependent anharmonic-vibrational correction given by^{68,71}

$$\Delta P = -\frac{\hbar}{4} \sum_i \frac{1}{\omega_i^2} \left(\frac{\partial P}{\partial Q_i} \right)_0 \sum_j \frac{K_{ij}}{\omega_j} \coth \frac{\hbar \omega_j}{2k_B T} + \frac{\hbar}{4} \sum_i \frac{1}{\omega_i} \left(\frac{\partial^2 P}{\partial Q_i^2} \right)_0 \coth \frac{\hbar \omega_i}{2k_B T} \quad (5)$$

From the equation above the dependence of vibrational corrections upon temperature T is apparent. According to eq 5, the quantities needed are the first and diagonal second derivatives of the molecular property P with respect to the mass-weighted normal modes evaluated at the equilibrium geometry of the molecule, the harmonic frequencies ω_p , and the cubic semidiagonal force constants K_{ij} . In passing, we note that a rotational term can be also included in eq 5 to take into account centrifugal-distortion effects.⁷²

Anharmonic Force Field. The computations of vibrational spectra beyond the double-harmonic approximation, the vibrational corrections to rotational constants and molecular properties, and the zero-point vibrational (ZPV) contributions to the conformational energy were obtained within the VPT2 approach.^{53,67,70,71,73–76} This provides a cost-effective route to compute accurate vibrational properties, at least for semirigid systems. However, it requires the problem of singularities, known as resonances, to be overcome. In the present work, we made use of the GVPT2 scheme, which consists of removing the resonant terms from the perturbed treatment and then treating them with a proper reduced-dimensionality variational approach. To identify the Fermi resonances, the criteria proposed by Martin et al.⁷⁷ were used. Similarly to vibrational frequencies, the equations of the transition integrals suffer from the presence of singularities due to Fermi resonances but also to 1–1 resonances. For Fermi resonances, the definition based on the test proposed by Martin et al.⁷⁷ was used, whereas for the 1–1 resonances⁷⁸ the definition proposed in ref 71 was adopted.

As already mentioned, the double-hybrid B2PLYP functional was employed in conjunction with the aug-cc-pVTZ basis set for the evaluation of the anharmonic force field. To further

Table 2. Equilibrium Structure (Distances in Å, Angles in degrees) and Dipole Moment (debye) of *cis*-Acrolein

| parameters | this work | | | experiment |
|----------------------|--------------------|----------------------------|----------------------------|-----------------------|
| | B2PLYP/aug-cc-pVTZ | best ^a estimate | semiexp ^b r_e | r_s^c |
| C1–O ₄ | 1.2139 | 1.2102 | 1.2101(3) | 1.215(6) |
| C1–C2 | 1.4810 | 1.4816 | 1.4818(4) | 1.478(6) |
| C2–C3 | 1.3336 | 1.3343 | 1.3359(4) | 1.340(7) |
| C1–H5 | 1.1040 | 1.1024 | 1.1020(3) | 1.106(4) |
| C2–H6 | 1.0823 | 1.0823 | 1.0814(3) | 1.088(4) |
| C3–H7 | 1.0812 | 1.0815 | 1.0810(5) | 1.098(5) |
| C3–H8 | 1.0797 | 1.0797 | 1.0791(3) | 1.081(3) |
| C2–C1–O ₄ | 124.49 | 123.97 | 123.88(3) | 124.2(4) |
| C3–C2–C1 | 121.83 | 121.21 | 121.28(3) | 121.5(6) |
| C2–C1–H5 | 116.85 | 115.83 | 115.82(4) | 1185.8(4) |
| C3–C2–H6 | 121.32 | 121.59 | 121.59(4) | 121.1(4) |
| C2–C3–H7 | 120.10 | 119.84 | 119.84(3) | 118.5(3) |
| C2–C3–H8 | 121.67 | 121.59 | 121.59(5) | 121.5(6) |
| μ_d | 2.762 | 2.639 ^d | | |
| μ_0^{298} | 2.708 | 2.585 ^e | | 2.552(3) ^f |

^aBest estimate from eq 1. ^b B_0 from ref 14 (parent species: ref 13) and vibrational corrections at the B2PLYP/aug-cc-pVTZ level. Given uncertainties are 3 times the standard deviation of the fit. ^cSubstitution structure ref 14. ^dEquilibrium values computed at the best-estimated structure using the CCSD(T)/aug-cc-pVQZ level of theory. ^eEquilibrium values of footnote *e* corrected for vibrational and temperature effects at the B2PLYP/aug-cc-pVTZ level. ^fReference 13.

improve the description of the latter, and provide accurate and cost-effective results, the hybrid CCSD(T)/B2PLYP approach (shortly denoted CC/DFT) was used, assuming that the differences in the anharmonic frequencies computed at the CCSD(T) and DFT levels are only due to the harmonic terms. The harmonic part of the force field was thus computed at the CCSD(T)/cc-pVTZ level (within the frozen-core approximation) using analytic second derivatives.^{79,80} The hybrid frequencies were then computed by means of a *posteriori* corrections to the harmonic CCSD(T) frequencies, $\omega(\text{CC})$:

$$\nu_{\text{CC/DFT}} = \omega(\text{CC}) + \Delta\nu_{\text{DFT}} \quad (6)$$

where $\Delta\nu_{\text{DFT}}$ are the anharmonic corrections at the B2PLYP/aug-cc-pVTZ. We rely on this approximation because it has already been validated for several closed- and open-shell systems (see for instance refs 81–85). Analogously, anharmonic hybrid CCSD(T)/DFT IR intensities were obtained by means of an *a posteriori* scheme, again assuming that the differences between the two levels of theory can only be ascribed to the harmonic part. Therefore, hybrid intensities were derived as

$$I_{\text{CC/DFT}}^{\text{anh}} = I^{\text{harm}}(\text{CC}) + \Delta I_{\text{DFT}}^{\text{anh}} \quad (7)$$

RESULTS AND DISCUSSION

The results for the molecular structure determination of *trans*- and *cis*-acrolein are summarized in Tables 1 and 2, respectively, with the atoms labeled according to Figure 1. First, we note that for both conformers the best-estimated theoretical (CCSD(T)/CBS+CV; eq 1) and semiexperimental parameters agree well within 0.001 Å for bond lengths and in most cases within 0.05 degrees for angles. This good agreement therefore confirms the typical accuracy for CCSD(T)/CBS+CV structures that can be inferred from the literature on this topic (see, for example, refs.^{28–30,33,86}), i.e., an accuracy of 0.001–0.002 Å for bond distances and about 0.05–0.1 degrees for angles. To the best of our knowledge, despite the number of theoretical investigations on acrolein and its *trans*–*cis* isomerization,^{16,21,23–27,87} the

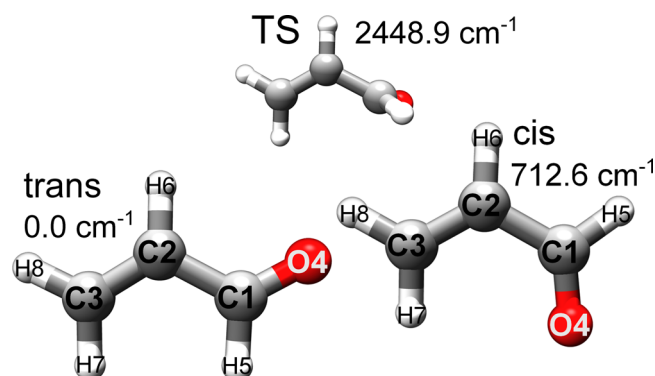


Figure 1. Molecular structure of *trans*- and *cis*-acrolein and the transition state for the *trans*–*cis* isomerization. Atoms labeling and relative energies.

present work is the first one addressing the issue of the molecular structure at such a high level of theory. For examples, in refs 26 and 87 CCSD(T)/cc-pVTZ, which is our starting level, was employed in structural and energetic determinations. Therefore, a comparison with previous studies is not too meaningful. On the other hand, it is worth noting the good performance of the computationally cheap B2PLYP/aug-cc-pVTZ level of theory. With the only exception of the C–O distance, the bond lengths agree within 0.001 Å, whereas for angles the agreement is on average within 0.2°.

Focusing on the semiexperimental equilibrium structure, which was obtained as explained in the methodology section, we note that for both *trans*- and *cis*-acrolein very good residuals were obtained: in terms of observed – calculated differences for equilibrium rotational constants, the root-mean-square (rms) deviation is ~0.0001 MHz for *trans* and ~0.0002 MHz for *cis*. We furthermore point out the importance of the electronic corrections to rotational constants, in particular for the *trans* form. In fact, these corrections only halve the inertial defects for the *cis* isotopologues, whereas they lower those of *trans* by 1 order of magnitude. For the latter conformer, this improvement has an important role in reducing the standard deviation of the

Table 3. Conformational, ΔE_{cis} , and Isomerization Energies, ΔE_{iso} ^a (Values in cm^{-1})

| level of theory - energy: | this work | | | | experiment |
|--|--------------------|--------------------|----------------|----------------------------|------------------------|
| | B2PLYP/aug-cc-pVTZ | CCSD(T)/CBS+CV | CCSD(T)/CBS+CV | best estimate ^b | |
| level of theory - geometry: | B2PLYP/aug-cc-pVTZ | B2PLYP/aug-cc-pVTZ | CCSD(T)/CBS+CV | CCSD(T)/CBS+CV | |
| ΔE_{cis} | 805.3 | 726.3 | 722.9 | 729.3 | |
| $\Delta E_{\text{cis}} + \text{ZPV}_{\text{harm}}^c$ | 791.8 | 712.9 | 709.4 | 715.8 | |
| $\Delta E_{\text{cis}} + \text{ZPV}_{\text{anh}}$ | 795.0 | 716.1 | 712.6 | 719.0 | 660 (40) ^d |
| ΔE_{iso} | 2915.1 | 2658.0 | | | |
| $\Delta E_{\text{iso}} + \text{ZPV}_{\text{harm}}^c$ | 2706.0 | 2448.9 | | | 2340, 600 ^e |

^a ΔE_{cis} means energy difference between the *cis* and *trans* forms. ΔE_{iso} means energy difference between the transition state and *trans*-acrolein. ^bBest-estimated energies from eq 4. ^cZPV corrections at the B2PLYP/aug-cc-pVTZ level. ^dReferences 8 and 22. ^eReference 26.

Table 4. Vibrational Frequencies (cm^{-1}) and IR Intensities (km mol^{-1}) of *trans*-Acrolein^a

| mode | sym | harmonic | | anharmonic | | experiment ^c | assignment |
|------|-----|--------------------|-----------------|--------------------|-------------------------------|-------------------------|---------------------------|
| | | B2PLYP/aug-cc-pVTZ | CCSD(T)/cc-pVTZ | B2PLYP/aug-cc-pVTZ | hybrid ^b CC/B2PLYP | | |
| 1 | A' | 3251.6 (3.6) | 3241.6 (5.0) | 3112.4 (5.4) | 3102.4 (6.8) | 3103 | CH ₂ assym str |
| 2 | A' | 3199.7 (0.9) | 3195.5 (1.0) | 3068.8 (3.6) | 3064.6 (3.7) | 3069 | HC(CO) str |
| 3 | A' | 3156.5 (4.4) | 3144.2 (4.4) | 3002.1 (6.1) | 2989.8 (6.1) | 2998 | CH ₂ sym str |
| 4 | A' | 2916.9 (83.0) | 2919.5 (82.9) | 2813.0 (90.0) | 2815.6 (89.9) | 2800 ^d | HC(CC) str |
| 5 | A' | 1746.0 (236.6) | 1763.9 (165.6) | 1709.7 (218.7) | 1727.6 (147.7) | 1724 | C=O str |
| 6 | A' | 1672.0 (3.5) | 1662.8 (3.6) | 1634.7 (1.9) | 1625.5 (2.0) | 1625 | C=C str |
| 7 | A' | 1463.4 (10.2) | 1457.3 (8.5) | 1424.1 (10.1) | 1418.0 (8.4) | 1420 | CH ₂ sciss |
| 8 | A' | 1392.7 (5.2) | 1391.2 (4.1) | 1364.8 (5.2) | 1363.3 (4.1) | 1360 | HC(CC) bend |
| 9 | A' | 1305.2 (2.6) | 1292.5 (3.2) | 1281.9 (2.0) | 1269.2 (2.6) | 1275 | HC(CO) bend |
| 10 | A' | 1179.8 (39.4) | 1170.6 (33.9) | 1155.2 (34.8) | 1144.0 (29.3) | 1158 | C—C str |
| 11 | A' | 927.3 (19.7) | 919.8 (16.8) | 914.1 (21.3) | 906.6 (18.4) | 912 | CH ₂ rock |
| 12 | A' | 572.1 (4.1) | 567.3 (4.2) | 566.1 (3.6) | 561.3 (3.7) | 564 | CCO bend |
| 13 | A' | 321.4 (10.4) | 314.2 (10.1) | 324.0 (8.9) | 313.2 (8.6) | 324 | CCC bend |
| 14 | A'' | 1026.8 (5.9) | 1024.7 (7.4) | 1012.3 (6.6) | 1010.2 (8.1) | 993 | C=C tors |
| 15 | A'' | 1038.2 (12.5) | 1009.9 (17.8) | 1016.5 (10.6) | 988.2 (15.9) | 972 | HC(CC) wag. |
| 16 | A'' | 1000.5 (37.4) | 974.5 (30.5) | 982.3 (36.8) | 956.3 (29.9) | 959 | CH ₂ wag. |
| 17 | A'' | 615.9 (10.3) | 606.3 (10.0) | 602.5 (9.6) | 592.9 (9.3) | 593 | HC(CO) wag. |
| 18 | A'' | 166.0 (4.6) | 163.0 (4.4) | 161.8 (4.5) | 158.8 (4.3) | 158 | C—C tors |

^aIR intensities are given in parentheses. ^bHybrid force field: harmonic part at the CCSD(T)/cc-pVTZ level, anharmonic corrections at the B2PLYP/aug-cc-pVTZ level. See text. ^cExperimental gas-phase IR spectrum from ref 18. ^dMode ν_4 involved in Fermi interactions with $2\nu_7$, $2\nu_8$, $\nu_7 + \nu_8$, and $\nu_5 + \nu_{10}$.

fit, and thus improving the results. All possible combinations of rotational constants (i.e., A and B, B and C, A and C) provide similar results in values and standard deviation. The geometrical parameters collected in Tables 1 and 2 are those from the combination A and C because this provides the smaller rms.

The last comment concerns the comparison of our best structures with the only pure experimental data available. In Tables 1 and 2, for comparison purposes, the substitution r_s structure¹⁴ is reported. As is well-known (see, for instance, ref 30), this type of geometry presents severe limitations in properly describing the equilibrium geometry. In the present case, the distances involving carbons and oxygen agree within the given uncertainties, which range from 0.004 to 0.007 Å. On the other hand, the C—H bond lengths are overestimated up to 0.017 Å.

Tables 1 and 2 also collect the equilibrium dipole moment computed at different levels of theory and the corresponding vibrationally corrected values (according to eq 5). We note a very good agreement of the CCSD(T)/aug-cc-pVQZ values with the experimental determination once the vibrational/temperature correction is included. The latter amounts to 0.1 debye for the *trans* conformer and to about 0.05 debye for *cis*, and in both cases it lowers the equilibrium values. Concerning

the B2PLYP/aug-cc-pVTZ level, we note that for both conformers it provides values overestimated by about 5%.

The energy difference between the *cis* and *trans* minima is given in Table 3 together with the interconversion barrier (ruled by the transition state, TS, shown in Figure 1).^a We first of all note that the B2PLYP/aug-cc-pVTZ level provides a good reference structure for accurate thermochemical computations; in fact, the best-estimated conformational energy (at the CBS+CV level; see methodology section) evaluated at the B2PLYP/aug-cc-pVTZ equilibrium geometry is overestimated by only 0.5% with respect to the analogous determination carried out using the best-estimated structure. This is an important result in view of accurate energetic characterization of medium- to large-sized molecules. We furthermore point out that B2PLYP permits us to obtain rather accurate energetic determinations: according to the results of Table 3, the B2PLYP/aug-cc-pVTZ level of theory provides conformational and isomerization energies overestimated by only 10%. This good accuracy is even more emphasized by the fact that the CCSD(T)/cc-pVTZ level of theory underestimates the conformational energy by about 13%. Equilibrium energy values are lowered by inclusion of ZPV corrections: by about 2% in the case of conformational energy and by about 8.5% for the isomerization barrier. As described in the Methodology section, to improve our

Table 5. Vibrational Frequencies (cm^{-1}) and IR Intensities (km mol^{-1}) of *cis*-Acrolein^a

| mode | sym | harmonic | | anharmonic | | experiment | | assignment |
|------|-----|--------------------|-----------------|--------------------|-------------------------------|------------------|-------------------|---------------------------|
| | | B2PLYP/aug-cc-pVTZ | CCSD(T)/cc-pVTZ | B2PLYP/aug-cc-pVTZ | hybrid ^b CC/B2PLYP | gas ^c | Ar ^d | |
| 1 | A' | 3261.8 (1.2) | 3252.9 (2.0) | 3122.5 (2.5) | 3113.6 (3.3) | | | CH ₂ assym str |
| 2 | A' | 3187.4 (9.6) | 3183.4 (9.3) | 3054.6 (12.7) | 3050.6 (12.4) | | | HC(CO) str |
| 3 | A' | 3165.1 (4.4) | 3154.1 (4.4) | 3060.1 (4.7) | 3049.1 (4.7) | | | CH ₂ sym str |
| 4 | A' | 2942.1 (126.30) | 2948.3 (122.7) | 2844.3 (122.1) | 2850.5 (118.5) | 2838 | 2848 ^e | HC(CC) str |
| 5 | A' | 1752.4 (96.3) | 1760.7 (79.3) | 1718.1 (84.2) | 1726.4 (67.2) | 1722 | 1724 | C=O str |
| 6 | A' | 1661.1 (75.1) | 1659.0 (41.3) | 1623.3 (65.1) | 1621.2 (31.3) | 1624 | 1616 | C=C str |
| 7 | A' | 1446.6 (42.2) | 1440.4 (37.6) | 1410.6 (42.2) | 1404.4 (37.6) | 1403 | 1406 | CH ₂ sciss |
| 8 | A' | 1431.0 (1.6) | 1430.0 (0.4) | 1400.6 (1.3) | 1399.6 (0.1) | | | HC(CC) bend |
| 9 | A' | 1319.6 (2.6) | 1306.5 (2.0) | 1294.0 (2.6) | 1280.9 (2.0) | 1285 | | HC(CO) bend |
| 10 | A' | 1075.0 (3.9) | 1064.9 (3.5) | 1058.1 (3.7) | 1048.0 (3.3) | 1056 | | C—C str |
| 11 | A' | 936.0 (61.5) | 933.6 (54.6) | 916.2 (60.4) | 913.8 (53.5) | 919 | 918 | CH ₂ rock |
| 12 | A' | 682.3 (12.0) | 676.9 (11.8) | 656.5 (11.2) | 651.1 (11.0) | 669 | | CCO bend |
| 13 | A' | 284.9 (6.8) | 284.6 (6.6) | 277.8 (6.3) | 277.5 (6.1) | 276 | | CCC bend |
| 14 | A'' | 1037.4 (4.6) | 1022.6 (6.1) | 1019.1 (8.3) | 1004.3 (9.8) | 1005 | | C=C tors |
| 15 | A'' | 1027.6 (36.2) | 1011.7 (31.6) | 1008.1 (27.5) | 994.2 (22.9) | 988 | 995 | HC(CC) wag. |
| 16 | A'' | 1014.0 (7.4) | 984.5 (10.6) | 996.9 (12.2) | 967.4 (15.4) | 970 | 970 | CH ₂ wag. |
| 17 | A'' | 559.6 (10.3) | 557.4 (10.3) | 547.2 (9.2) | 549.4 (9.2) | 544 | 547 | HC(CO) wag. |
| 18 | A'' | 141.0 (6.5) | 152.8 (6.2) | 140.7 (5.8) | 152.5 (5.5) | 138 | | C—C tors |

^aIR intensities are given in parentheses. ^bHybrid force field: harmonic part at the CCSD(T)/cc-pVTZ level, anharmonic corrections at the B2PLYP/aug-cc-pVTZ level. See text. ^cExperimental gas-phase IR spectrum from ref 17. ^dExperimental low-temperature Ar Matrix spectrum, assigned tentatively to *cis*-acrolein in ref 10. ^eMode ν_4 involved in Fermi interactions with $2\nu_8$ at 2729 cm^{-1} (2730 cm^{-1} B3PLYP), experimental value reported in ref 10 of 2756 cm^{-1} .

determination, the contribution of full treatment of triples and the effects of quadruple excitations were considered. The corresponding corrections are $+2.66$ and $+3.75 \text{ cm}^{-1}$, respectively, thus leading to our best estimate (also including ZPV) for the *cis*–*trans* energy difference: 719.0 cm^{-1} . This value can be compared with the available experimental value.^{8,22} We note a reasonably good agreement with the latter (i.e., within twice the experimental uncertainty $\sim 40 \text{ cm}^{-1}$), our computed value being only $\sim 60 \text{ cm}^{-1}$ ($\sim 10\%$) larger. This discrepancy is very small ($0.17 \text{ kcal mol}^{-1} = 0.72 \text{ kJ mol}^{-1}$) and tends to confirm the accuracy of the composite scheme employed (see, for example, ref 33). Future experimental investigations might further confirm the accuracy of our determination. In the literature, experimental estimates for the isomerization barrier are also available (for a thorough discussion, the reader is referred to ref 26), but the corresponding determination is affected by several uncertainties. Therefore, a comparison between theory and experiment for ΔE_{iso} is not too meaningful, and we thus recommend our best-estimated value to be used as reference.

Moving to the discussion of the vibrational spectra, the harmonic and anharmonic fundamental frequencies of *trans*- and *cis*-acrolein together with the corresponding IR intensities are collected in Tables 4 and 5, respectively. We first note that the B2PLYP/aug-cc-pVTZ level provides harmonic frequencies very similar to the CCSD(T)/cc-pVTZ ones; in fact, the mean deviation is only about 0.51% (9.6 cm^{-1}), with the large discrepancy being in relative terms $\sim 7\%$ (maximum absolute deviation: 29.5 cm^{-1}). Such an agreement thus supports the *a posteriori* approximation employed for deriving the hybrid force field. We furthermore note that the largest discrepancies are observed for the normal modes of A'' symmetry. If only the A' modes are considered, the averaged discrepancy reduces to 7.0 cm^{-1} , with the maximum deviation being 17.9 cm^{-1} . This effect might be ascribed to a slower convergence of perturbative treatment of electron correlation in the case of modes affected

by conjugation. As mentioned in the computational details section, the B2PLYP/aug-cc-pVTZ level of theory has been chosen for its proved accuracy. It is therefore not surprising that, when we move to the comparison with experiment, mean absolute deviations (MAEs) of 9.7 and 6.3 cm^{-1} are observed for B2PLYP/aug-cc-pVTZ and the hybrid force field, respectively. As already noted for the harmonic terms, the modes of A'' symmetry are those affected by larger deviations. In fact, the MAEs of the two computational models agree within about 1 cm^{-1} for the modes of A' symmetry, whereas for the A'' ones the correction of the harmonic frequencies at the CCSD(T)/cc-pVTZ level within hybrid schemes leads to an improvement of 12.7 and 7.5 cm^{-1} for *trans* and *cis* conformers, respectively.

As evident from Tables 4 and 5, almost all experimental fundamental frequencies are well reproduced by our computations, but additional comments are warranted for vibrations around 2800 cm^{-1} , where several Fermi resonances involving the ν_4 fundamental (assigned to the HC(CC) stretching) are observed for both conformers. For *trans*-acrolein, the resonances involving ν_4 are with $2\nu_7$ (2833 cm^{-1}), $2\nu_8$ (2679 cm^{-1}), $\nu_7 + \nu_8$ (2757 cm^{-1}), and $\nu_5 + \nu_{10}$ (2874 cm^{-1}), but only one transition was experimentally assigned in this spectral region. At variance, two transitions at 2756 and 2848 cm^{-1} , observed in low-temperature Ar matrix experiment upon irradiation,¹⁰ were assigned to the *cis*-acrolein. According to our computations, they can be assigned to the components of the $\nu_4 \approx 2\nu_8$ Fermi polyad, with the $2\nu_8$ overtone predicted at 2729 cm^{-1} by the hybrid force field (2730 cm^{-1} B2PLYP). The good agreement between computation and experiment for all vibrations reported in ref 10 further confirms their tentative assignment to the *cis*-acrolein. In passing, we note that for *trans*-acrolein, several fundamental and nonfundamental transitions were assigned in high-resolution (HR) measurements,^{19,20} which confirmed the values reported in Table 4. Concerning overtones and combination bands, experimental data for *trans*-

acrolein (on which HR measurements were focused on) agree well with our computations: 313 and 324 cm^{-1} for $2\nu_{18}$, 484 and 488 cm^{-1} for $\nu_{18} + \nu_{13}$, 650 and 654 cm^{-1} for $2\nu_{13}$, respectively. This agreement further confirms the accuracy of our computations also for nonfundamental transitions. Thus, theoretical results reported in the present work for *trans*-acrolein nonfundamental transitions in 2600–2900 cm^{-1} spectral range may facilitate assignment of future measurements.

The last comment concerns IR intensities. From Tables 4 and 5, it is evident that also for these quantities, B2PLYP/aug-cc-pVTZ and CCSD(T)/cc-pVTZ provide similar results.

CONCLUDING REMARKS

In the present paper a thorough investigation of the equilibrium structure of the *trans* and *cis* forms of acrolein is reported. For the first time, their molecular structure has been determined by means of high-level quantum-chemical calculations at the coupled-cluster level, thus providing structural parameters with an estimated accuracy of about 0.001 Å for bond distances and of about 0.05° for angles. The pure computational determination has also been complemented by a semixperimental approach, which is based on the combination of experimental ground-state rotational constants with calculated vibrational corrections. This is nowadays considered the best approach to determine reliable equilibrium geometries for polyatomic molecules (see for instance refs 30, 38, and 39).

The conformational *trans*–*cis* energy and the barrier for the corresponding isomerization have been determined by means of a composite scheme that systematically extrapolates ab initio energies, accounts for electron correlation through coupled cluster theory, including up to single, double, triple, and quadruple excitations, and furthermore corrects for core–electron correlation and anharmonic zero-point vibrational energy. Such an investigation confirms that the *trans* conformer is only about 700 cm^{-1} more stable than *cis*. Our best-estimated isomerization barrier, 2449 cm^{-1} (7 kcal mol^{-1}), can be considered the most accurate and reliable determination available so far.

With respect to the spectroscopic characterization, it has been further confirmed that the hybrid CC/DFT approach applied to the GVPT2 computations yields anharmonic wavenumbers with an accuracy of about 10 cm^{-1} , in all spectral regions and also for nonfundamental transitions. Moreover, the present results allowed us to confirm the tentative assignment of IR transitions, observed upon irradiation of *trans*-acrolein deposited in low-temperature Ar matrix, to *cis*-acrolein, and to assign the features at 2756 and 2848 cm^{-1} to the components of $\nu_4 \simeq 2\nu_8$ Fermi polyad.

In conclusion, the present study further confirms that high-level quantum-chemical computations with an adequate treatment of electron correlation effects, extrapolation to the basis-set limit and inclusion of core correlation are able to quantitatively predict molecular structures and spectroscopic parameters and thus provide important benchmark data to either validate or predict experimental information.

ASSOCIATED CONTENT

Supporting Information

The Cartesian coordinates of the structures of the three stationary points optimized at the B2PLYP/aug-cc-pVTZ level together with those of the *trans* and *cis* forms at the CCSD(T)/

CBS+CV level. This material is available free of charge via the Internet at <http://pubs.acs.org>.

AUTHOR INFORMATION

Corresponding Authors

*C. Puzzarini: e-mail, cristina.puzzarini@unibo.it.

*V. Barone: e-mail, vincenzo.barone@sns.it.

Notes

The authors declare no competing financial interest.

ACKNOWLEDGMENTS

This work was supported by Italian MIUR (PRIN 2012 “STAR: Spectroscopic and computational Techniques for Astrophysical and atmospheric Research” and PON 1078) and by the University of Bologna (RFO funds). The high performance computer facilities of the DREAMS center (<http://dreamshpc.sns.it>) are acknowledged for providing computer resources. The support of COST CMTS-Action CM1002 “CONvergent Distributed Environment for Computational Spectroscopy (CODECS)” is also acknowledged. The research leading to these results has received funding from the European Union’s Seventh Framework Programme (FP7/2007-2013) under grant agreement No. ERC-2012-AdG-320951-DREAMS.

ADDITIONAL NOTE

^aThe Cartesian coordinates of the structures of the three stationary points optimized at the B2PLYP/aug-cc-pVTZ level are given in the Supporting Information together with those of the *trans* and *cis* forms at the CCSD(T)/CBS+CV level.

REFERENCES

- (1) Arntz, D.; Fischer, A.; Hoepp, M.; Jacobi, S.; Sauer, J.; Ohara, T.; Sato, T.; Shimizu, N.; Schwind, H. *Acrolein and Methacrolein*; Wiley-VCH Verlag GmbH & Co. KGaA: Weinheim, Germany, 2012.
- (2) Hollis, J. M.; Jewell, P. R.; Lovas, F. J.; Remijan, A.; Möllendal, H. Green Bank Telescope Detection of New Interstellar Aldehydes: Propenal and Propanal. *Astrophys. J.* **2004**, *610*, L21–L24.
- (3) Cherniak, E. A.; Costain, C. C. Microwave Spectrum and Molecular Structure of *trans*-Acrolein. *J. Chem. Phys.* **1966**, *45*, 104–110.
- (4) Wagner, R.; Fine, J.; Simmons, J. W.; Goldstein, J. H. Microwave Spectrum, Structure, and Dipole Moment of *s*-*trans* Acrolein. *J. Chem. Phys.* **1957**, *26*, 634–637.
- (5) Harris, R. K. Vibrational assignments for glyoxal, acrolein and butadiene. *Spectrochim. Acta* **1964**, *20*, 1129–1141.
- (6) Brand, J. C. D.; Williamson, D. G. Near-ultra-violet spectrum of propenal. *Discuss. Faraday Soc.* **1963**, *35*, 184–191.
- (7) Harris, R. K. The electronic absorption spectrum of acrolein vapour. *Spectrochim. Acta* **1963**, *19*, 1425–1426 E1–E2, 1427–1441.
- (8) Alves, A. C. P.; Christoffersen, J.; Hollas, J. M. Near ultra-violet spectra of the *s*-*trans* and a second rotamer of acrolein vapour. *Mol. Phys.* **1971**, *20*, 625–644.
- (9) Alves, A. C. P.; Christoffersen, J.; Hollas, J. M. Near ultra-violet spectra of the *s*-*trans* and a second rotamer of acrolein vapour. *Mol. Phys.* **1971**, *21*, 384.
- (10) Krantz, A.; Goldfarb, T. D.; Lin, C. Y. Simple method for assigning vibrational frequencies to rapidly equilibrating rotational isomers. *J. Am. Chem. Soc.* **1972**, *94*, 4022–4024.
- (11) Blom, C. E. *S*-*trans* and *S*-*cis* acrolein: trapping from thermal molecular beams and uv-induced isomerization in argon matrices. *Chem. Phys. Lett.* **1980**, *73*, 483–486.
- (12) Carreira, L. A. Raman spectrum and torsional potential function of acrolein. *J. Phys. Chem.* **1976**, *80*, 1149–1152.

- (13) Blom, C. E.; Bauder, A. Microwave spectrum, rotational constants and dipole moment of *s*-cis acrolein. *Chem. Phys. Lett.* **1982**, *88*, 55–58.
- (14) Blom, C. E.; Grassi, G.; Bauder, A. Molecular structure of *s*-cis and *s*-trans-acrolein determined by microwave spectroscopy. *J. Am. Chem. Soc.* **1984**, *106*, 7427–7431.
- (15) Winnewisser, M.; Winnewisser, G.; Honda, T.; Hirita, E. Ground State Centrifugal Distortion Constants of Trans-Acrolein, CH₂=CH-CHO from the Microwave and Millimeter Wave Rotational Spectra. *Z. Naturforsch.* **1975**, *30*, 1001–1014.
- (16) Jaman, A. J.; Bhattacharya, R. Millimeter-Wave Rotational Spectra of trans-Acrolein (Propenal) (CH₂CHCOH): A DC Discharge Product of Allyl Alcohol (CH₂CHCH₂OH) Vapor and DFT Calculation. *J. Atomic Mol., Opt. Phys.* **2012**, *2012*, No. 363247.
- (17) Osborne, G. A.; Ramsay, D. A. Near Ultraviolet Absorption Spectra of cis and trans Acrolein and Acrolein-d₁. *Can. J. Phys.* **1973**, *51*, 1170–1175.
- (18) Hamada, Y.; Nishimura, Y.; Tsuboi, M. Infrared spectrum of trans-acrolein. *Chem. Phys.* **1985**, *100*, 365–375.
- (19) McKellar, A. R. W.; Tokaryk, D. W.; Appadoo, D. R. T. The far-infrared spectrum of acrolein, CH₂CHCHO: The ν_{18} fundamental and ($\nu_{17}+\nu_{18}$)- ν_{18} hot bands. *J. Mol. Spectrosc.* **2011**, *244*, 146–152.
- (20) Xu, L.-H.; Jiang, X.-J.; Shi, H.-Y.; Lees, R. M.; McKellar, A. R. W.; Tokaryk, D. W.; Appadoo, D. R. T. 10 μ m High-resolution spectrum of trans-acrolein: Rotational analysis of the ν_{11} , ν_{16} , ν_{14} and $\nu_{16} + \nu_{18} - \nu_{18}$ bands. *J. Mol. Spectrosc.* **2011**, *268*, 136–146.
- (21) Celebre, G.; Concistré, M.; Luca, G. D.; Longeri, M.; Pileio, G.; Emsley, J. W. The Structure of Acrolein in a Liquid Crystal Phase. *Chemistry* **2005**, *11*, 3599–3608.
- (22) Bair, E. J.; Goetz, W.; Ramsay, D. A. Magnetic Rotation and Absorption Spectra of cis and trans Acrolein. *Can. J. Phys.* **1971**, *49*, 2710–2717.
- (23) Page, C. S.; Olivucci, M. Ground and excited state CASPT2 geometry optimizations of small organic molecules. *J. Comput. Chem.* **2003**, *24*, 298–309.
- (24) Aquilante, F.; Barone, V.; Roos, B. O. A theoretical investigation of valence and Rydberg electronic states of acrolein. *J. Chem. Phys.* **2003**, *119*, 12323–12334.
- (25) Saha, B.; Ehara, M.; Nakatsuji, H. Singly and doubly excited states of butadiene, acrolein, and glyoxal: Geometries and electronic spectra. *J. Chem. Phys.* **2006**, *125*, 014316.
- (26) Bokareva, O. S.; Bataev, V. A.; Godunov, I. A. A quantum-chemical study of the structure and conformational dynamics of the acrolein molecule in the ground electronic state. *Russ. J. Phys. Chem.* **2009**, *83*, 81–90.
- (27) Guareschi, R.; Filippi, C. Ground- and Excited-State Geometry Optimization of Small Organic Molecules with Quantum Monte Carlo. *J. Chem. Theory Comput.* **2013**, *9*, 5513–5525.
- (28) Heckert, M.; Kállay, M.; Gauss, J. Molecular equilibrium geometries based on coupled-cluster calculations including quadruple excitations. *Mol. Phys.* **2005**, *103*, 2109–2115.
- (29) Heckert, M.; Kállay, M.; Tew, D. P.; Klopper, W.; Gauss, J. Basis-set extrapolation techniques for the accurate calculation of molecular equilibrium geometries using coupled-cluster theory. *J. Chem. Phys.* **2006**, *125*, 044108.
- (30) Puzzarini, C.; Stanton, J. F.; Gauss, J. Quantum-chemical calculation of spectroscopic parameters for rotational spectroscopy. *Int. Rev. Phys. Chem.* **2010**, *29*, 273–367.
- (31) Carrington, T.; Wang, X.-G. Computing ro-vibrational spectra of van der Waals molecules. *Wiley Interdiscip. Rev.: Comput. Mol. Sci.* **2011**, *1*, 952–963.
- (32) Tennyson, J. Accurate variational calculations for line lists to model the vibration-rotation spectra of hot astrophysical atmospheres. *Wiley Interdiscip. Rev.: Comput. Mol. Sci.* **2012**, *2*, 698–715.
- (33) Barone, V.; Biczysko, M.; Bloino, J.; Puzzarini, C. The performance of composite schemes and hybrid CC/DFT model in predicting structure, thermodynamic and spectroscopic parameters: the challenge of the conformational equilibrium in glycine. *Phys. Chem. Chem. Phys.* **2013**, *15*, 10094–10111.
- (34) Puzzarini, C.; Biczysko, M.; Barone, V.; Largo, L.; Peña, I.; Cabezas, C.; Alonso, J. L. Accurate Characterization of the Peptide Linkage in the Gas Phase: A Joint Quantum-Chemical and Rotational Spectroscopy Study of the Glycine Dipeptide Analogue. *J. Phys. Chem. Lett.* **2014**, *5*, 534–540.
- (35) Barone, V.; Baiardi, A.; Biczysko, M.; Bloino, J.; Cappelli, C.; Lipparini, F. Implementation and validation of a multi-purpose virtual spectrometer for large systems in complex environments. *Phys. Chem. Chem. Phys.* **2012**, *14*, 12404–12422.
- (36) Barone, V.; Biczysko, M.; Bloino, J. Fully anharmonic IR and Raman spectra of medium-size molecular systems: accuracy and interpretation. *Phys. Chem. Chem. Phys.* **2014**, *16*, 1759–1787.
- (37) Pulay, P.; Meyer, W.; Boggs, J. E. Cubic force constants and equilibrium geometry of methane from Hartree–Fock and correlated wavefunctions. *J. Chem. Phys.* **1978**, *68*, 5077–5085.
- (38) Pawłowski, F.; Jørgensen, P.; Olsen, J.; Hegelund, F.; Helgaker, T.; Gauss, J.; Bak, K. L.; Stanton, J. F. Molecular equilibrium structures from experimental rotational constants and calculated vibration–rotation interaction constants. *J. Chem. Phys.* **2002**, *116*, 6482–6496.
- (39) Demaison, J. Experimental, semi-experimental and ab initio equilibrium structures. *Mol. Phys.* **2007**, *105*, 3109–3138.
- (40) Jaeger, H. M.; Schaefer, H. F., III; Demaison, J.; Császár, A. G.; Allen, W. D. Lowest-Lying Conformers of Alanine: Pushing Theory to Ascertain Precise Energetics and Semiexperimental r_e Structures. *J. Chem. Theory Comput.* **2010**, *6*, 3066–3078.
- (41) Raghavachari, K.; Trucks, G. W.; Pople, J. A.; Head-Gordon, M. A fifth-order perturbation comparison of electron correlation theories. *Chem. Phys. Lett.* **1989**, *157*, 479–483.
- (42) Dunning, T. H., Jr. Gaussian basis sets for use in correlated molecular calculations. I. The atoms boron through neon and hydrogen. *J. Chem. Phys.* **1989**, *90*, 1007–1023.
- (43) Kendall, A.; Dunning, T. H., Jr.; Harrison, R. J. Electron affinities of the first-row atoms revisited. Systematic basis sets and wave functions. *J. Chem. Phys.* **1992**, *96*, 6796–6806.
- (44) Woon, D. E.; Dunning, T. H., Jr. Gaussian basis sets for use in correlated molecular calculations. V. Core-valence basis sets for boron through neon. *J. Chem. Phys.* **1995**, *103*, 4572–4585.
- (45) Stanton, J. F.; Gauss, J.; Harding, M. E.; Szalay, P. G. CFour A quantum chemical program package. 2011; with contributions from A. Auer, R. J. Bartlett, U. Benedikt, C. Berger, D. E. Bernholdt, Y. J. Bomble, O. Christiansen, M. Heckert, O. Heun, C. Huber, T.-C. Jagau, D. Jonsson, J. Jusélius, K. Klein, W. J. Lauderdale, D. Matthews, T. Metzroth, L. A. Mueck, D. P. O’Neill, D. R. Price, E. Prochnow, C. Puzzarini, K. Ruud, F. Schiffmann, W. Schwalbach, S. Stopkowicz, A. Tajti, J. Vázquez, F. Wang, J. D. Watts and the integral packages MOLEUCLE (J. Almlöf and P. R. Taylor), PROPS (P. R. Taylor), ABACUS (T. Helgaker, H. J. Aa. Jensen, P. Jørgensen, and J. Olsen), and ECP routines by A. V. Mitin and C. van Wuelen. For the current version, see <http://www.cfour.de> (accessed September 13, 2012).
- (46) Grimme, S. Semiempirical hybrid density functional with perturbative second-order correlation. *J. Chem. Phys.* **2006**, *124*, 034108.
- (47) Schwabe, T.; Grimme, S. Double-hybrid density functionals with long-range dispersion corrections: higher accuracy and extended applicability. *Phys. Chem. Chem. Phys.* **2007**, *9*, 3397–3406.
- (48) Biczysko, M.; Panek, P.; Scalmani, G.; Bloino, J.; Barone, V. Harmonic and Anharmonic Vibrational Frequency Calculations with the Double-Hybrid B2PLYP Method: Analytic Second Derivatives and Benchmark Studies. *J. Chem. Theory Comput.* **2010**, *6*, 2115–2125.
- (49) Frisch, M. J.; et al. *Gaussian 09*, Revision D.01; 2009; Gaussian Inc.: Wallingford, CT, 2009.
- (50) Feller, D. The use of systematic sequences of wave functions for estimating the complete basis set, full configuration interaction limit in water. *J. Chem. Phys.* **1993**, *98*, 7059–7071.
- (51) Helgaker, T.; Klopper, W.; Koch, H.; Noga, J. Basis-set convergence of correlated calculations on water. *J. Chem. Phys.* **1997**, *106*, 9639–9646.
- (52) Peterson, K. A.; Dunning, T. H. Accurate correlation consistent basis sets for molecular core-valence correlation effects: The second

row atoms Al-Ar, and the first row atoms B-Ne revisited. *J. Chem. Phys.* **2002**, *117*, 10548–10560.

(53) Mills, I. M. In *Molecular Spectroscopy: Modern Research*; Rao, K. N., Mathews, C. W., Eds.; Academic: New York, 1972.

(54) Flygare, W. H. Magnetic interactions in molecules and an analysis of molecular electronic charge distribution from magnetic parameters. *Chem. Rev.* **1974**, *74*, 653.

(55) Gordy, W.; Cook, R. L. In *Microwave Molecular Spectra*, 3rd ed.; Weissberger, A., Ed.; Wiley: New York, 1984.

(56) Tajti, A.; Szalay, P. G.; Császár, A. G.; Kállay, M.; Gauss, J.; Valeev, E. F.; Flowers, B. A.; Vázquez, J.; Stanton, J. F. HEAT: High accuracy extrapolated *ab initio* thermochemistry. *J. Chem. Phys.* **2004**, *121*, 11599–11613.

(57) Császár, A. G.; Allen, W. D.; Schaefer, H. F., III. In pursuit of the *ab initio* limit for conformational energy prototypes. *J. Chem. Phys.* **1998**, *108*, 9751–9764.

(58) Karton, A.; Rabinovich, E.; Martin, J. M. L.; Ruscic, B. W4 theory for computational thermochemistry: In pursuit of confident sub-kJ/mol predictions. *J. Chem. Phys.* **2006**, *125*, 144108.

(59) Peterson, K. A.; Feller, D.; Dixon, D. A. Chemical accuracy in *ab initio* thermochemistry and spectroscopy: current strategies and future challenges. *Theor. Chem. Acc.* **2012**, *131*, 1079.

(60) Noga, J.; Bartlett, R. J. The full CCSDT model for molecular electronic structure. *J. Chem. Phys.* **1987**, *86*, 7041.

(61) Scuseria, G. E.; Schaefer, H. F., III. A new implementation of the full CCSDT model for molecular electronic-structure. *Chem. Phys. Lett.* **1988**, *152*, 382–386.

(62) Watts, J. D.; Bartlett, R. J. The coupled-cluster single, double, and triple excitation model for open-shell single reference functions. *J. Chem. Phys.* **1993**, *93*, 6104.

(63) Kállay, M.; Gauss, J. Approximate treatment of higher excitations in coupled-cluster theory. *J. Chem. Phys.* **2005**, *123*, 214105/1–13.

(64) Kállay, M.; Gauss, J. Approximate treatment of higher excitations in coupled-cluster theory. II. Extension to general single-determinant reference functions and improved approaches for the canonical Hartree-Fock case. *J. Chem. Phys.* **2008**, *129*, 144101/1–9.

(65) Kállay, M. MRCC, a generalized CC/CI program. For the current version, see <http://www.mrcc.hu>.

(66) Schuurman, M. S.; Allen, W. D.; von Ragué Schleyer, P.; Schaefer, H. F., III. The highly anharmonic BH₃ potential energy surface characterized in the *ab initio* limit. *J. Chem. Phys.* **2005**, *122*, 104302.

(67) Bloino, J.; Biczysko, M.; Barone, V. General Perturbative Approach for Spectroscopy, Thermodynamics, and Kinetics: Methodological Background and Benchmark Studies. *J. Chem. Theory Comput.* **2012**, *8*, 1015–1036.

(68) Mort, B. C.; Autschbach, J. Magnitude of Zero-Point Vibrational Corrections of Optical Rotation in Rigid Organic Molecules. *J. Phys. Chem. A* **2005**, *109*, 8617–8623.

(69) Barone, V. Vibrational zero-point energies and thermodynamic functions beyond the harmonic approximation. *J. Chem. Phys.* **2004**, *120*, 3059–3065.

(70) Barone, V. Anharmonic vibrational properties by a fully automated second-order perturbative approach. *J. Chem. Phys.* **2005**, *122*, 014108.

(71) Bloino, J.; Barone, V. A second-order perturbation theory route to vibrational averages and transition properties of molecules: General formulation and application to infrared and vibrational circular dichroism spectroscopies. *J. Chem. Phys.* **2012**, *136*, 124108.

(72) Jameson, C. J. Variation of chemical shielding with internal coordinates. Applications to diatomic molecules. *J. Chem. Phys.* **1977**, *66*, 4977–4982.

(73) Nielsen, H. H. The Vibration-Rotation Energies of Molecules. *Rev. Mod. Phys.* **1951**, *23*, 90–136.

(74) Isaacson, A. D.; Truhlar, D. G.; Scanlon, K.; Overend, J. Tests of approximation schemes for vibrational energy levels and partition functions for triatomics: H₂O and SO₂. *J. Chem. Phys.* **1981**, *75*, 3017–3024.

(75) Amos, R. D.; Handy, N. C.; Green, W. H.; Jayatilaka, D.; Willets, A.; Palmieri, P. Anharmonic vibrational properties of CH₂F₂: A comparison of theory and experiment. *J. Chem. Phys.* **1991**, *95*, 8323–8336.

(76) Vázquez, J.; Stanton, J. F. Simple(r) algebraic equation for transition moments of fundamental transitions in vibrational second-order perturbation theory. *Mol. Phys.* **2006**, *104*, 377–388.

(77) Martin, J. M. L.; Lee, T. J.; Taylor, P. R.; Francois, J.-P. The anharmonic force field of ethylene, C₂H₄, by means of accurate *ab initio* calculations. *J. Chem. Phys.* **1995**, *103*, 2589–2602.

(78) Bloino, J.; Guido, C.; Lipparini, F.; Barone, V. A fully automated implementation of VPT2 Infrared intensities. *Chem. Phys. Lett.* **2010**, *496*, 157–161.

(79) Gauss, J.; Stanton, J. Analytic CCSD(T) second derivatives. *Chem. Phys. Lett.* **1997**, *276*, 70.

(80) Szalay, P. G.; Gauss, J.; Stanton, J. F. Analytic UHF-CCSD(T) second derivatives: implementation and application to the calculation of the vibration-rotation interaction constants of NCO and NCS. *Theor. Chim. Acta* **1998**, *100*, 5–11.

(81) Begue, D.; Carbonniere, P.; Pouchan, C. Calculations of Vibrational Energy Levels by Using a Hybrid *ab Initio* and DFT Quartic Force Field: Application to Acetonitrile. *J. Phys. Chem. A* **2005**, *109*, 4611–4616.

(82) Carbonniere, P.; Lucca, T.; Pouchan, C.; Rega, N.; Barone, V. Vibrational computations beyond the harmonic approximation: performances of the B3LYP functional for semirigid molecules. *J. Comput. Chem.* **2005**, *26*, 384–388.

(83) Puzzarini, C.; Barone, V. Toward spectroscopic accuracy for organic free radicals: Molecular structure, vibrational spectrum, and magnetic properties of F₂NO. *J. Chem. Phys.* **2008**, *129*, 084306/1–7.

(84) Puzzarini, C.; Barone, V. Assessment of a computational strategy approaching spectroscopic accuracy for structure, magnetic properties and vibrational frequencies of organic free radicals: the F₂CN and F₂BO case. *Phys. Chem. Chem. Phys.* **2008**, *10*, 6991–6997.

(85) Puzzarini, C.; Biczysko, M.; Barone, V. Accurate Harmonic/Anharmonic Vibrational Frequencies for Open-Shell Systems: Performances of the B3LYP/N07D Model for Semirigid Free Radicals Benchmarked by CCSD(T) Computations. *J. Chem. Theory Comput.* **2010**, *6*, 828–838.

(86) Puzzarini, C.; Heckert, M.; Gauss, J. The accuracy of rotational constants predicted by high-level quantum-chemical calculations. I. molecules containing first-row atoms. *J. Chem. Phys.* **2008**, *128*, 194108/1–9.

(87) Shishkina, S. V.; Slabko, A. I.; Shishkin, O. V. Conjugation vs hyperconjugation in molecular structure of acrolein. *Chem. Phys. Lett.* **2013**, *556*, 18–22.